

# INTER-UNIVERSITY ACCELERATOR CENTER

---

## Magnetic Field profiling of a quadrupole

---

*Author:*

Arnab BARMAN RAY  
Indian Institute Of  
Technology Kharagpur

*Supervisors:*

Dr. Abani MANDAL  
Mr. Sarvesh KUMAR

1st June - 29th June 2015



# Contents

1	Introduction	3
2	Transform Matrix Formalism	5
3	Ampere turn calculations	6
4	Coil Design For a Quadrupole	7
5	Simulations using Opera-3D	8
6	Experimental Results	10
7	Summary Of Experiments	15
8	References & Acknowledgement	15

## List of Figures

1	Physical Model of the quadrupole . . . . .	4
2	Amperian Loop . . . . .	7
3	Pyramid structure of winding wires . . . . .	8
4	Quadrupole Model . . . . .	9
5	Vector field in iron core . . . . .	9
6	Vector field in air . . . . .	10
7	$B_y$ along $z$ (simulation) . . . . .	11
8	Calibration of the electromagnet . . . . .	12
9	$B_y$ along $z$ (experiment) . . . . .	14

## Abstract

Magnetic quadrupoles are used as focusing devices in accelerators. They focus ion beams using intense magnetic fields which decreases the cross-section of the beam as it passes through. In this project, experiments were carried out to determine the magnetic centre of a quadrupole among other important parameters. Simulations in Opera3D were used to understand the field distribution within the device.

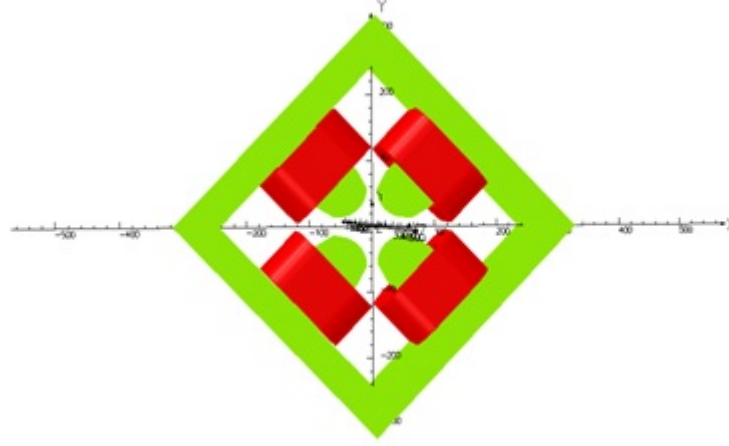
## 1 Introduction

Quadrupoles are, as the name suggests, magnetic arrangements consisting of four poles, which are usually two north and two south poles with like poles opposite to one another. They are primarily used for focusing ion beams in accelerators. The magnetic field inside a quadrupole is such that ions travelling along the axis perpendicular to the plane of the quadrupole experience magnetic forces which results in either convergence or divergence of the beam depending on which plane the ion is travelling in. A single quadrupole focuses the ion beam in one plane while defocusing the same in another plane. . When two quadrupoles are used in a doublet, they focus the beam in both the planes, but the degree of convergence in the two cannot be made the same. This gives rise to aberrations in the ion beam. Magnification is not equal in both the transverse planes. To solve this problem of astigmatism, another quadrupole is used alongwith the doublet, resulting in a triplet of quadrupoles. A triplet can be used to achieve equal magnification in both the planes. Hence a sharply focussed beam is obtained. In this project, a quadrupole was experimentally investigated to obtain some important parameters. Also, simulations in opera 3d were carried out to compare the accuracy of the results, e.g measurement of effective length, magnetic centre and excitation studies.

The region inside a quadrupole is current free. As a result the magnetic field is irrotational. That is,  $\nabla \times \vec{B} = 0$ . Hence,  $\vec{B}$  can be represented using a magnetic scalar potential  $\phi$  so that  $\vec{B} = \nabla\phi$ , which using the earlier condition gives rise to the equation:

$$\nabla^2\phi = 0 \tag{1}$$

25/Jun/2015 19:12:54



UNITS	
Length	mm
Magn Flux Density T	A m <sup>-1</sup>
Magn Field	A m <sup>-1</sup>
Magn Scalar Pot.	A
Magn Vector Pot.	Wb m <sup>-1</sup>
Elec Flux Density	C m <sup>-1</sup>
Elec Field	V m <sup>-1</sup>
Conductivity	S m <sup>-1</sup>
Current Density	A mm <sup>2</sup>
Power	W
Force	N
Energy	J
Mass	kg
MODEL DATA	
quadropole real simulation final.op3	
TOSCA Magnetostatic	
Linear materials	
Simulation No 1 of 1	
13524038 elements	
2808755 nodes	
4 conductors	
Nodally interpolated fields	
Activated in global coordinates	
Field Point Local Coordinates	
Local = Global	

Opera

Figure 1: Physical Model of the quadrupole

This gives the general solution for the potential as:

$$\phi(r, \theta) = a_0 + b_0 \log r + \sum_{n=0}^{\infty} (Ar^n + Br^{-n})(C \cos n\theta + D_n \sin n\theta) \quad (2)$$

where the constants,  $a_0$  and  $b_0$  are evaluated using the boundary conditions.

For a quadrupole with circular pole faces, and axes oriented as shown in the Figure 1: The field is given as:

$$B_x = -B_0 \frac{y}{a} \text{ and } B_y = -B_0 \frac{x}{a} \quad (3)$$

or in polar coordinates, they are given as:

$$B_r = -B_0 \frac{r \sin 2\theta}{a} \text{ and } B_\theta = B_0 \frac{r \cos 2\theta}{a} \quad (4)$$

An interesting observation is that along a circle of a radius  $R$  the magnitude of the magnetic field is:

$$|\vec{B}| = \sqrt{B_x^2 + B_y^2} = B_0 \frac{R}{a}$$

is constant along the circle.

This result is re-obtained using Opera 3d simulations in section 5.

## 2 Transform Matrix Formalism

The use of transform matrices in ray optics is well known. Each optical component, which is usually a lens is described by a matrix which acts on the light beam coordinates(before the lens) and gives the coordinates of the beam after it's emergence from the component. In beam optics too, the use of transform matrices is widespread. Each element, whether magnetic or electrostatic in nature, is described by a  $2 \times 2$  or  $3 \times 3$  matrix. The nature of the use is described below. A beam is characterized by six parameters :  $x, x', y, y', z$  and  $p_z$ . The axis of propagation of the beam is considered to be along  $z$ -axis.  $x'$  and  $y'$  are coordinates which describe the momentum along the  $x$  and  $y$  directions respectively. These are called the divergences of the beam.  $x'$  is defined as:  $p_x/p_z$ , while  $y'$  is :  $p_y/p_z$ .

Usually,  $p_z \gg p_x$  or  $p_y$ , giving  $x' \ll 1$  and  $y' \ll 1$ . If space charge is neglected, which is a pretty good approximation for high energy beams, the phase space can be independently described by  $x, x'$  and  $y, y'$ , separate from  $z$  and  $p_z$ (in case dispersion is small). Each lens in the beam transport system is independently characterized by certain matrices in the  $xz$  and  $yz$  planes separately. A lens characterized by the matrix  $A$  in the  $yz$  planes acts on a beam coordinate as follows:

$$\begin{pmatrix} y_2 \\ y'_2 \end{pmatrix} = \begin{pmatrix} a_{11} & a_{12} \\ a_{21} & a_{22} \end{pmatrix} \begin{pmatrix} y_1 \\ y'_1 \end{pmatrix} \quad (5)$$

Where  $(y_1 y'_1)$  is the vector in the  $yy'$  part of the six dimensional phase space, before the beam passes through the lens, while  $(y_2 y'_2)$  describes the beam in after it has passed through the lens.

Similarly, a different matrix is used to describe the transformation in the  $xz$ -plane. It is to be noted that the matrix representation of the lens rests on the so-called **Hard-Edge** model. It usually does not consider edge effects where the field is distorted.

### Transfer Matrix For a Quadrupole

The equations of motion of ion particles in a quadrupole is:

$$m\ddot{x} = -\frac{qv_z B_0}{a} \quad m\ddot{y} = -\frac{qv_z B_0}{a} y \quad (6)$$

Where  $B$  is the field strength at point on the surface of any of the poles closest to the origin  $a$  is the radius of the biggest circle inside the quadrupole

and  $q$  is the charge on the ion. The quadrupole focuses in the  $xz$  plane and defocuses in the  $yz$  plane. When the differentiation is carried out with respect to  $z$ , the equations are:

$$m\ddot{x} = -\frac{qv_z B_0}{a} \quad m\ddot{y} = -\frac{qv_z B_0}{a}y \quad (7)$$

The boundary conditions are:

$$y(0) = y_1, y(l) = y_2 \quad x(0) = x_1, x(l) = x_2 \quad l \text{ is the effective length of the quadrupole}$$

With these, the transfer-matrices take the form:

$$\begin{pmatrix} y_2 \\ y_2' \end{pmatrix} = \begin{pmatrix} \cosh kl & k^{-1} \sinh kl \\ k \sinh kl & \cosh kl \end{pmatrix} \begin{pmatrix} y_1 \\ y_1' \end{pmatrix} \quad \begin{pmatrix} x_2 \\ x_2' \end{pmatrix} = \begin{pmatrix} \cosh kl & k^{-1} \sinh kl \\ -k \sinh kl & \cosh kl \end{pmatrix} \begin{pmatrix} x_1 \\ x_1' \end{pmatrix} \quad (8)$$

where  $k = \sqrt{\frac{qB_0}{v_z a}}$ .

### 3 Ampere turn calculations

A coil having  $N$  turns is wound across each of the four poles, carrying the current  $I$  in such a way that we get two oppositely placed north and south poles respectively.

To calculate the value of  $B_0$  using an ampere loop, we choose the loop  $C_1$  to be as shown in the figure below. Along the loop,  $\oint_{C_1} \vec{H} \cdot d\vec{l} = NI$  where  $N$  is the number of turns wound around each coil and  $I$  is the current flowing through it. The field along BC is neglected because the relative permeability for iron  $\mu_r \approx 5000$ , which is very large. Using the field deduced in the first section we get

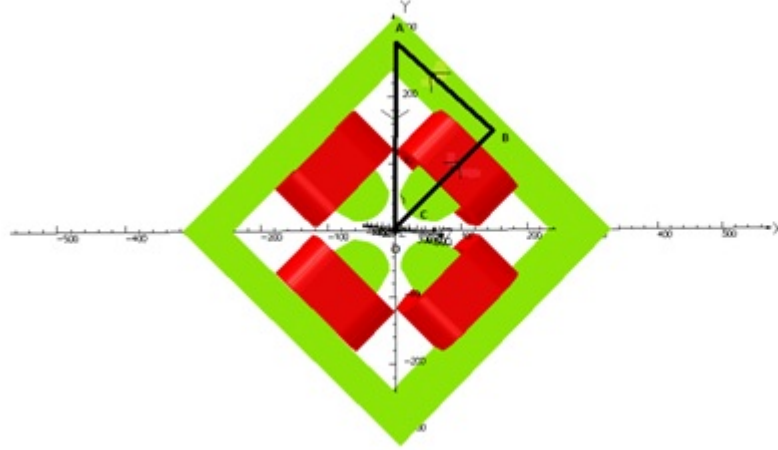
$$\int_0^a \frac{B_0 r}{a} dr = \mu NI$$

From this we get the magnetic gradient or  $B_0/a$ , or

$$g = \frac{2\mu_0 NI}{a^2} \quad (9)$$

For our quadrupole, we get  $N = 408$ ,  $a = 39$  mm and  $I$  is usually taken to be 6 A. Using these values  $g = 4.0450$  T/m. At  $I = 4.77$  A we get  $g = 3.2158$  T/m

25/Jun/2015 19:12:54



UNITS	
Length	mm
Magn Flux Density T	A m <sup>-1</sup>
Magn Field	A m <sup>-1</sup>
Magn Scalar Pot	A
Magn Vector Pot	Wb m <sup>-1</sup>
Elec Flux Density	C m <sup>-1</sup>
Elec Field	V m <sup>-1</sup>
Conductivity	S m <sup>-1</sup>
Current Density	A mm <sup>-2</sup>
Power	W
Force	N
Energy	J
Mass	kg

---

MODEL DATA	
quadrupole real simulation final.op3	
TOSCA Magnetostatic	
Linear materials	
Simulation No 1 of 1	
15024039 elements	
2808753 nodes	
4 conductors	
Nodally interpolated fields	
Activated in global coordinates	

---

Field Point Local Coordinates	
Local = Global	

Opera

Figure 2: Amperian Loop

## 4 Coil Design For a Quadrupole

The coil is wrapped around the pole in a brick-layered like structure. The number of windings from one end of the pole to the other end decreases steadily in the form: 33, 32, 31... all the way to 18 turns at the end where chamfer of the pole exists, as is shown in the Figure 2.

The total number of turns is:  $33+32+31+\dots+19+18 = 408$ , SWG number of wire used = 12. Height of pole = 78 mm. Diameter of wire = 2.6416 mm. Field Gradient of Quadrupole Magnet =  $B_{max}/a = 0.15/0.039 = 3.85$  T/m. Using the result (3) of the previous section, we calculate the value of  $NI$  as follows:

$$NI = \frac{ga^2}{2\mu_0} = 2331 \text{ Amp turns}$$

If we take Current  $I = 6$  A. Then  $N = 408$  turns per pole. The physical length of the quadrupole along the  $z$ -direction is given from the effective length by the equation,

$$L_{iron} = L_{eff} - 0.9R = 156 - 0.9 * 39 = 120.9 \text{ mm}$$

Pole Tip Radius = 1.134,  $R = 42.94$  mm. Height of coil along pole =  $33 \times 2.6415 = 87.1728$  mm Now we distribute the  $N = 408$  turns on the



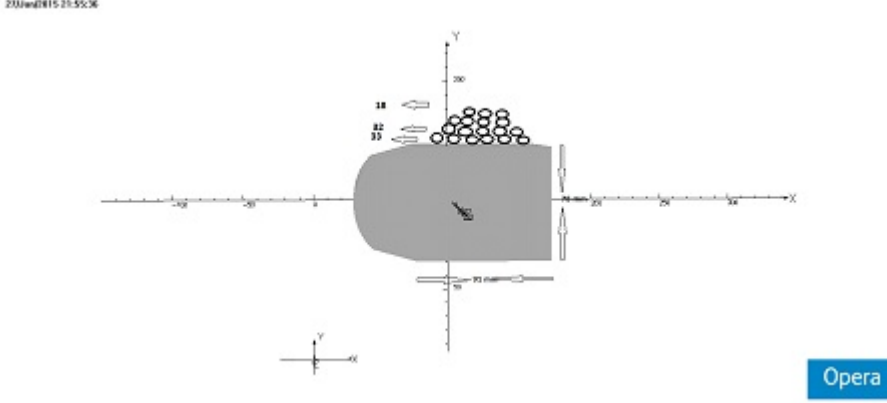


Figure 3: Pyramid structure of winding wires

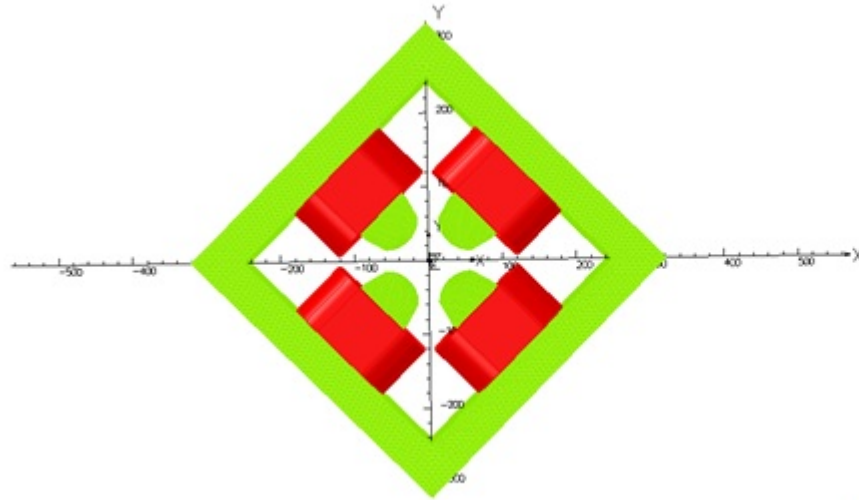
poles in 16 layers as 33, 32, 31, 30, 29, 28, 27, 26, 25, 24, 23, 22, 21, 20, 19, 18 as the no. of turns in respective layers. Average Length of the copper wire per turn =  $2(121 + 29 + 29 + 78) = 514$ . Total Length of Copper Wire per pole =  $514 \times 408 = 209712 \text{ mm} = 210 \text{ m} = 0.210 \text{ km}$ . From the resistivity of copper, the total resistance of the magnetic quadrupole is calculated to be  $2.64 \Omega$ . This is of the same order as the experimentally measured value of  $0.8 \Omega$ .

## 5 Simulations using Opera-3D

Opera 3-D is a modelling and simulation software used to solve magnetic and electric problems using the finite element method. Here, we import a pole made from Solidworks into Opera and then design the various other components of the Quadrupole. We use an approximation of racetrack conductors to simulate the magnetic field inside the quadrupole. The model and various parameters are shown in Figure 4. The analysis database is then created using a mesh size of 6 and an absolute tolerance of  $10^{-6}$ . The vector nature of the field inside the iron yoke of the quadrupole is shown using a vector field plot. The resultant model is shown in Figure 5.

The North and South poles are marked **N** and **S** respectively. A contour plot of the field in the inside region of the quadrupole is then shown in Figure 6. As is expected, the field is constant along circles as is expected from the theoretical result of **Section 1**. Value of the effective length is then estimated

25/Jun/2015 19:41:48



UNITS	
Length	mm
Magn Flux Density T	
Magn Field	A m <sup>-1</sup>
Magn Scalar Pot	A
Magn Vector Pot	Wb m <sup>-1</sup>
Elec Flux Density	C m <sup>-2</sup>
Elec Field	V m <sup>-1</sup>
Conductivity	S mm <sup>-1</sup>
Current Density	A mm <sup>-2</sup>
Power	W
Force	N
Energy	J
Mass	kg

MODEL DATA	
quadrupole real simulation final.op3	
TOSCA Magnetostatic	
Linear materials	
Simulation No 1 of 1	
15024039 elements	
2808755 nodes	
4 conductors	
Nodally interpolated fields	
Activated in global coordinates	

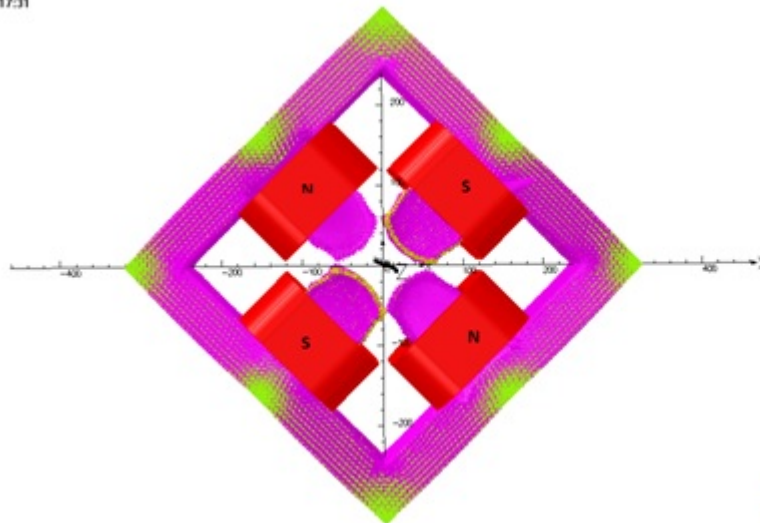
  

Field Point Local Coordinates	
Local = Global	

Opera

Figure 4: Quadrupole Model

25/Jun/2015 19:17:31



UNITS	
Length	mm
Magn Flux Density T	
Magn Field	A m <sup>-1</sup>
Magn Scalar Pot	A
Magn Vector Pot	Wb m <sup>-1</sup>
Elec Flux Density	C m <sup>-2</sup>
Elec Field	V m <sup>-1</sup>
Conductivity	S mm <sup>-1</sup>
Current Density	A mm <sup>-2</sup>
Power	W
Force	N
Energy	J
Mass	kg

MODEL DATA	
quadrupole real simulation final.op3	
TOSCA Magnetostatic	
Linear materials	
Simulation No 1 of 1	
15024039 elements	
2808755 nodes	
4 conductors	
Nodally interpolated fields	
Activated in global coordinates	

Field Point Local Coordinates	
Local = Global	

Opera

Figure 5: Vector field in iron core

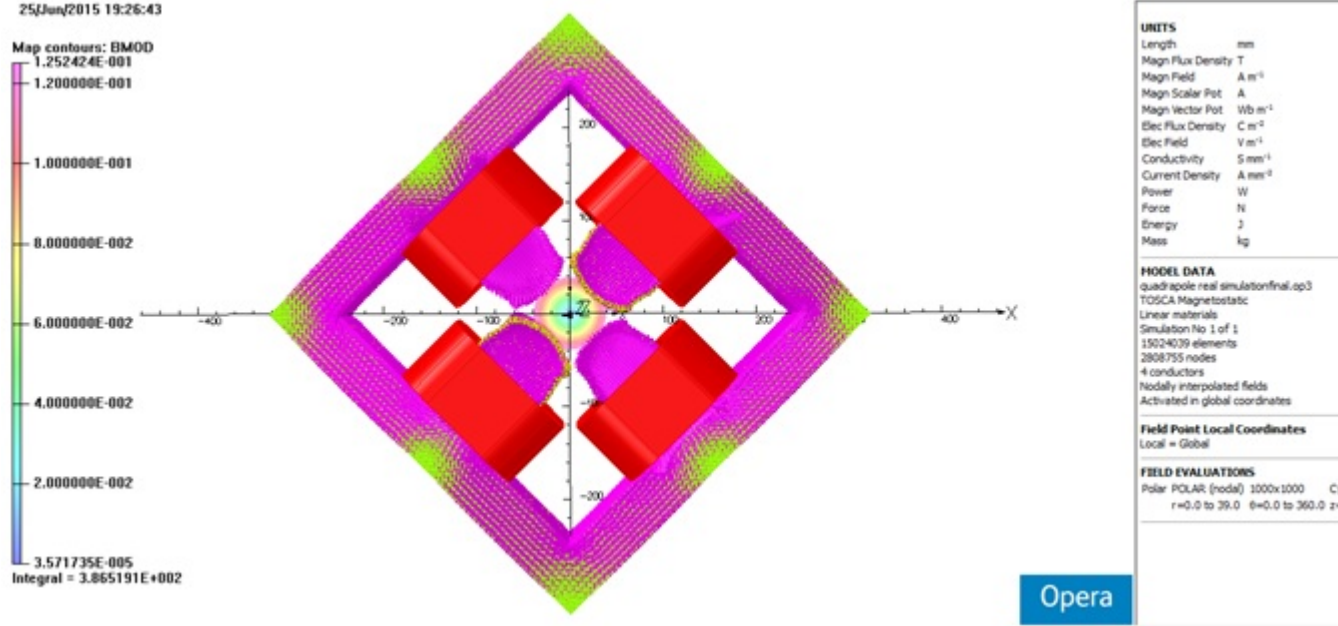


Figure 6: Vector field in air

using the magnetic field component variation along a line directed along the  $Z$ -axis as shown below: Plotting  $B_y$  along the line gives the graph in Figure 7.

The simulation gives an effective length of:

$$l_{eff} = 157.67 \text{ mm}$$

## 6 Experimental Results

The resistance of each of the magnets in the quadrupole is measured to be 0.8 ohm.

### Excitation studies

A Magnet Power Supply unit is used to supply current to the Quadrupole magnet. The current is measured using a multimeter to measure the voltage

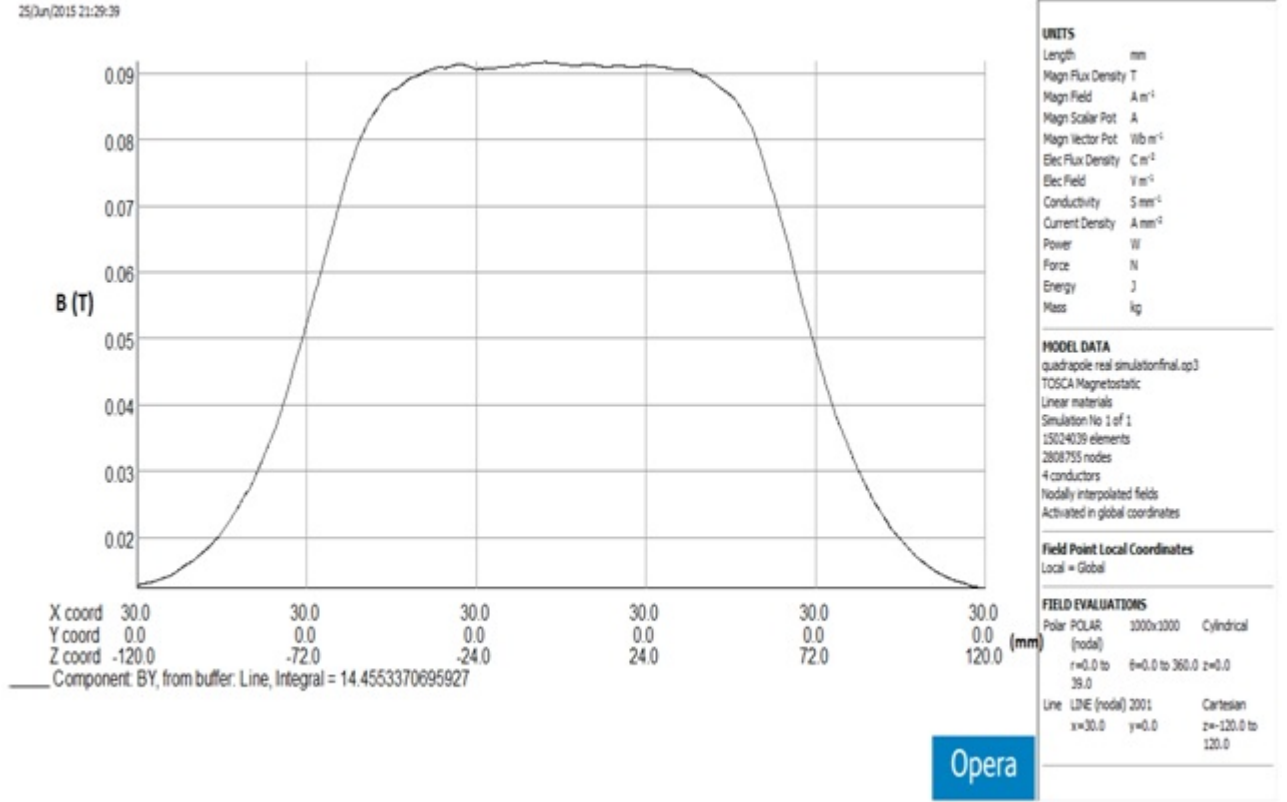


Figure 7:  $B_y$  along  $z$ (simulation)

across a shunt of known resistance 0.1 ohm, connected in series with the quadrupole. The current is then varied across different values and the magnetic field at the surface of one of the poles is measured using a Hall Probe and a Teslameter. The resulting plot and the theoretically expected line is shown in Figure 8. We use the parameters:  $N = 408$  and  $a = 39$  mm

## Magnetic Centre Measurement

Magnetic Centre is the point at which the Magnetic field of the Quadrupole is zero. Ideally, the quadrupole in question should have the centre at (0 mm, 0 mm). The deviation from this is a measure of the symmetry of the quadrupole. An aluminium cylinder with a rotating handle and a groove for the probe is rotated inside the quadrupole so that the magnetic field readings at each of the

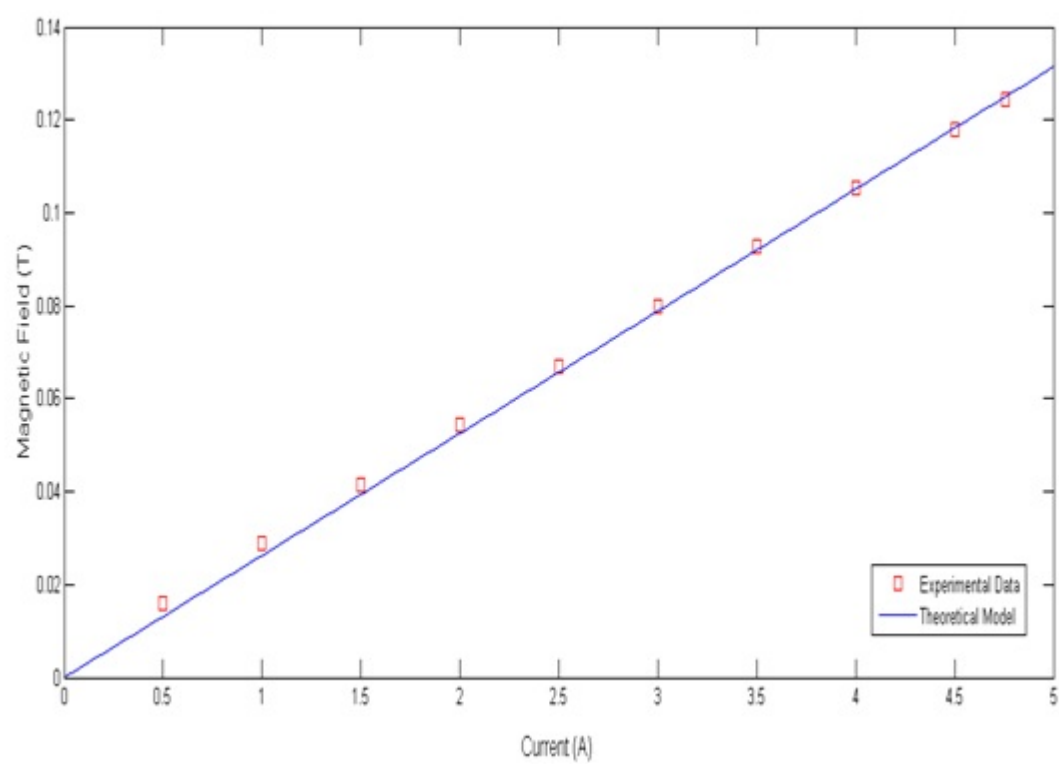


Figure 8: Calibration of the electromagnet

Radius (mm)	$B_x^+(T)$	$B_x^-(T)$	$M_x^-(mm)$	$B_y^-(T)$	$B_y^+(T)$	$M_y^-(T)$
33.12	0.0994150	0.0976600	0.292	-0.1099430	-0.1097080	-0.035
33.12	0.0994150	0.0982200	0.199	-0.1100500	-0.1097080	-0.052
33.12	-0.1105700	-0.109	0.2755757	0.0992390	0.0987620	-0.080
33.12	-0.1105700	-0.109	0.2201610	0.0993000	0.0987620	-0.090

Table 1: Data

Transformed $M_x(mm)$	Transformed $M_y(mm)$
0.232	0.182
0.177	0.104
0.251	0.138
0.219	0.092

Table 2: Magnetic centres

poles are measured at a current of 4.77 A. The values are found using two separate methods, in one of which we obtain the reading at the middle of the pole surface, while in another we take the maximum value of the field by making small deviations from the central pole surface. Throughout the experiment, care is taken not to move the cylinder in the longitudinal direction. The coordinates of the magnetic centre so obtained is transformed using an appropriate rotation matrix. The datasheet is given below: The coordinate system with X and Y axis along the poles is rotated by 45 degrees to give us the normal magnet system. The transformed magnetic centre coordinates are given as:

The first two rows give the magnetic field values at a current of 4.77 A, with the “middle” and “maximum” method respectively. The last two rows experience a current of  $-4.77$  A, with the 3rd row following the “middle” method and the 4th following the “maximum” method. The “middle” method is however, usually deemed to be more accurate. Hence, the two measured coordinates of the magnetic centre are: (0.232 mm , 0.181 mm) and (0.251 mm , 0.138 mm) As expected, the magnetic centre is very close to the origin and within 0.3 mm in any direction.

## Effective Length Measurements

An XYZ profiler is used to probe the magnetic field of the quadrupole. The Hall probe is secured tightly on the cantilever beam of the profiler. The

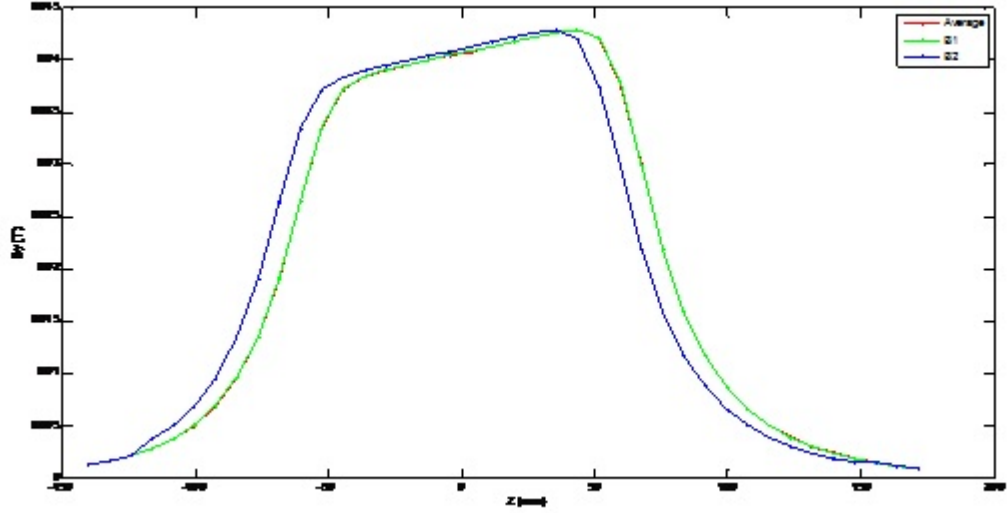


Figure 9:  $B_y$  along  $z$ (experiment)

profiler is then operated from a desktop computer where it is moved by 8 mm in each step in the  $Z$  direction, i.e along the axis of the quadrupole axis. The probe is situated at about 13 mm along the  $x$ -axis. The resulting  $Y$ (vertical) component magnetic field is measured with a Teslameter.

The measurement is taken from  $-140.5$  mm to  $164.5$  mm for two times( $B1$  and  $B2$ ) at a constant current of 4.77 A. Where 0 mm corresponds to the geometric centre of the quadrupole. The measured values as well as the averaged values are plotted on the graph below: The effective length from each of them through each of the methods applied to obtain the area under the curve is as follows:

**Trapezoidal Method:**

Average: 150.33 mm B1: 149.98 mm B2: 150.46 mm

**Rectangular Method(division by Max B):**

Average: 150.55 mm B1: 150.19 mm B2: 150.67 mm

**Rectangular Method(division by middle B):**

Average: 156.38 mm B1: 156.05 mm B2: 156.49 mm

**Reasons for tilt in the middle of the above graph:**

The quadrupole is not perfectly aligned with the XYZ scanner. So we are not sure whether it is exactly parallel to pole surface or not. The tilt confirms that the probe is at some angle rather than being tangential to the pole.

## 7 Summary Of Experiments

Parameters $M_x(\text{mm})$	Results $M_y(\text{mm})$
Magnetic Center	(0.232 mm, 0.181 mm) and (0.251 mm, 0.138 mm)
Effective Length	156.49 mm
Maximum Field @ 4.77 A	0.12 Tesla
Magnetic Field Gradient g@ 4.77 A	3.2158 T/m

Table 3: Magnetic centres

## 8 References & Acknowledgement

I have referred to the following books and resources during the project

- Weidmann - Particle Accelerator Physics I
- A.P. Banford – The Transport of Charged Particle Beams
- NSC school on accelerator physics 1988-89

I have received the kind and dedicated guidance of Dr. Sarvesh Kumar and Dr. Abani Mandal of Inter-University Accelerator Centre, New Delhi while doing experiments and clearing doubts about the theoretical basis of quadrupoles. I would like to express my heartfelt gratitude towards them. I would also like to thank my fellow students at IUAC summer programme for many fruitful discussions.